

Research Article

Asynchronous Two-Way Ranging Using Tomlinson-Harashima Precoding and UWB Signaling

Chih-Yu Wen,¹ Jun-Koh Chen,¹ and William A. Sethares²

¹The Department of Electrical Engineering, Graduate Institute of Communication Engineering, National Chung Hsing University, Taichung 402, Taiwan

²The Department of Electrical and Computer Engineering, University of Wisconsin-Madison, Madison, 1415 Engineering Drive, Madison, WI 53706-1691, USA

Correspondence should be addressed to Author please provide, Author please provide

Received 22 August 2007; Revised 9 November 2007; Accepted 7 January 2008

Recommended by Biao Chen

This paper demonstrates two methods which simultaneously undertake synchronization and ranging based on a time-of-arrival approach with bidirectional communication to bypass the need for accurate synchronous clocking. In order to alleviate multipath effects, Tomlinson-Harashima precoding and UWB signaling are used to measure the distance between pairs of sensors. The proposed schemes are shown to be effective under certain assumptions and the analysis is supported by simulation and numerical studies.

Copyright © 2008 Chih-Yu Wen et al. This is an open access article distributed under the Creative Commons Attribution License, which permits unrestricted use, distribution, and reproduction in any medium, provided the original work is properly cited.

1. INTRODUCTION

1 In many sensor network applications, it is useful or even required for sensors to be aware of their locations [1–5]. Due to the low-power, lower-cost, and simple configuration requirements of wireless sensor networks, GPS devices, accurate synchronous clocks, and manually configuring location information into each sensor during deployment may be precluded. However, accurate relative location estimates are achievable by relying on precise distance measurements between neighboring sensors [6–13].

Previous work [14] suggests that bidirectional signaling can be used to bypass the use of expensive clocks, but the analysis is limited by the assumption that only the line-of-sight (LOS) path exists. However, in real radio channels, there may exist multiple transmission paths between the sensors. In order to investigate the effect of this multipath interference on the distance estimations, this paper augments the previous schemes by utilizing channel estimation [15, 16], a Tomlinson-Harashima (TH) precoding (the modulo inverse filter [17]), and ultra-wideband (UWB) signaling for distance measurement in static multipath channels based on the time-of-arrival (TOA) methodology. Two distributed solutions are described for distance estimation in ad-hoc sen-

sor networks: (1) asynchronous ranging via TH precoding (ARTHP) and (2) asynchronous ranging via ultra-wideband (ARUWB). For the ARTHP method, channel information and a modulo inverse filter are used to combat the multipath effect and maximize the correlator output so that the estimator can carry out the range measurement accurately (detailed in Section 2). For the ARUWB method, the two-way UWB communication system is used to provide precise TOA estimates in multipath channels (detailed in Section 3). In this paper, the two proposed solutions integrate time synchronization, information processing, and ranging task to complete joint synchronization and ranging for wireless ad-hoc sensor networks with two-way communications.

Preequalization techniques are used principally in data transmission systems to combat the effect of interference caused by nonideal (multipath) channels. This paper proposes the application of TH precoding to the estimation of distance between pairs of sensors using bidirectional communication links over multipath channels. Assume that the channel characteristics do not vary significantly with time. Therefore, given the channel state information in the transmitter, it is possible to precode the information prior to transmission such that the problems which are generally inherent with the equalization at the receiver, such as the noise

2

enhancement, can be avoided. The key point in TH precoding is the nonlinear modulo-arithmetic operation to guarantee the stability of the precoder.

TH precoding is derived from linear preequalization at the transmitter. Disregarding the modulo congruence, TH precoding transforms the ISI channel $H(z)$ to a memoryless one and the system overall behavior is well approximated by the AWGN model. In [18, 19] a new precoding technique, called flexible precoding (FLP) or distribution-preserving precoding, is proposed. Unlike TH precoding, FLP resembles linear equalization at the receiver. The disadvantage of linear equalization is that noise is filtered with $1/H(z)$ and the desired precoding gain is lost. Compared with FLP, the performance of TH precoding has lower precoding loss and the implementation of TH precoding has simpler circuitry complexity. However, TH precoding requires the channel knowledge, which may limit its usage in randomly time-varying wireless channels. To avoid this drawback, a feedback channel, which continuously updates the channel state information, may be applied. These feedback channels are usually available in standardized wireless communication systems.

For TH precoding, the following are three possible scenarios. In the first, the transmitter and receiver share the same incorrect channel state information. In the second, the receiver has perfect channel knowledge but the transmitter has an incorrect channel estimate. In the third, channel state information is only available at the transmitter. In this work, given a pair of sensors, sensor A, and sensor B, the third scenario is considered where sensor B estimates the channel using a training sequence sent by sensor A, inverts the channel impulse response, and then sends the preequalized signal back to sensor A. This allows sensor A to accurately estimate the distance. Current literature on ranging using preequalization techniques for wireless sensor networks is limited. Related work in different precoding scenarios can be found in [20–26] and the references therein.

Besides the preequalization technique, a two-way TOA-based ranging technique with UWB signaling is proposed and the performance on ranging in UWB systems is studied. UWB radiolocation functionality usually relies on the ability to perform precise estimates of the TOA. Different TOA estimation methods for UWB propagation signals are investigated in [27–32]. Notice that the above research on ranging in UWB systems focuses on simulation and measurements of UWB ranging and positioning or on theoretical accuracy of UWB synchronization and ranging for UWB signals with no specific application IEEE 802.15.3a/4a [33–35] signal formats. On the other hand, the CRLBs for several UWB signal formats are derived to complement the previous literature on UWB ranging by providing a theoretical framework for the analysis of achievable ranging accuracy [36]. In addition, a global distributed solution is proposed to enable the simultaneous performance of time synchronization and positioning in UWB ad-hoc networks [37]. It is demonstrated that a cooperative and distributed maximization of the log-likelihood of range estimates can reduce the uncertainty on estimated positions in comparison with classical distributed weighted least squares approaches. However, the analysis in [36] is impractical since it does not take the effect of clock parameters

into account. In [37], although the described solution considers the clock-dependent ranging error, the operation of the proposed synchronization scheme and the diffusion algorithm that ensures the convergence of clock parameters are complex for ad-hoc networks.

In general, ranging accuracy depends on precise time synchronization, time stamp reading, and information management such as computation and signal processing. This paper presents an estimation-theoretic analysis of the proposed measurement mechanisms to assess the achievable estimation accuracy. Two main ranging errors are considered: (1) the clock-dependent ranging error and (2) the signal-to-noise- (SNR-) dependent ranging error. These two ranging errors are examined carefully to assess their impact on the TOA ranging accuracy.

The rest of the paper is organized as follows. Section 2 describes the ARTHP method and analyzes the ranging accuracy. Section 3 presents the ARUWB approach and assesses the estimation accuracy for both AWGN and multipath channels. Then, Section 4 addresses the performance of the proposed ranging approaches and discusses the trade-offs between ARTHP and ARUWB in terms of energy consumption, circuitry and computational complexity, and ranging accuracy. Finally, Section 5 draws conclusions and shows future research directions.

2. ASYNCHRONOUS RANGING VIA TH PRECODING (ARTHP)

This section describes the Asynchronous Ranging via TH Precoding (ARTHP) technology to examine the effect of multipath interference on ranging problems. The proposed method outlines one way to estimate the distance using channel estimation and the notion of cooperation between pairs of wireless sensors. Given two sensors A and B, sensor A initiates communication by sending a training sequence. Then, sensor B carries out a channel estimation based on maximizing the output of the correlator. Based on channel estimation, sensor B generates a modified training sequence for correlating with the training sequence sent from sensor A. Once sensor B detects the peak of the correlator output, it triggers a time counter and initiates the TH precoding. After receiving the signal from sensor B, sensor A stops the timer based on the performance of the correlator output and calculates the propagation time t_{ab} . Thus, sensor B estimates the channel and applies the TH precoding using a training sequence sent by sensor A, and allows A to accurately estimate the distance. The basic principle of the ARTHP method is captured in Figure 1.

- (i) Sensor A sends training sequence $s(t)$ for channel estimation and time synchronization in sensor B.
- (ii) Sensor B carries out a channel estimation based on maximizing the output of the correlator and time synchronization using the time stamps of transmission and reception in sensors A and B.
- (iii) Based on the channel estimation, sensor B generates a modified training sequence $y_2(t)$ that can be used to

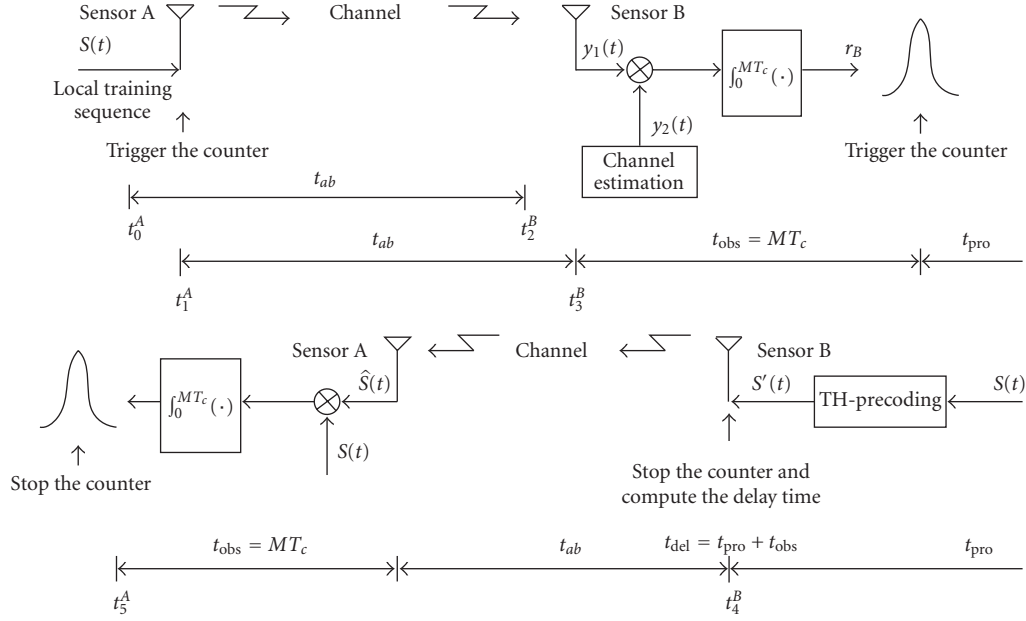


FIGURE 1: The ARTHP method: block diagram of a bidirectional communication and distance measurement system using channel estimation and TH precoding.

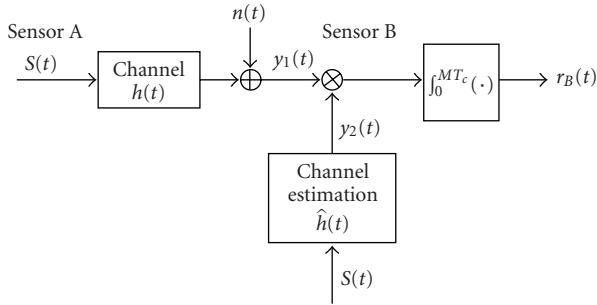


FIGURE 2: The correlator structure using channel information.

correlate with the received training sequence $y_1(t)$ sent from A. The correlator output of sensor B, $r_B(t)$, is

$$r_B = \int_0^{MT_c} y_1(t)y_2(t)dt, \quad (1)$$

where T_c represents the time interval between symbols and MT_c is the correlation time.

- (iv) Once sensor B detects the peak of the correlator output, it triggers a time counter, initiates the TH precoding, and records the processing delay. Then, sensor B transmits the preequalized signal and the delay information back to sensor A.
- (v) After receiving the signal from sensor B, sensor A stops the timer based on the performance of the correlator output and calculates the propagation time t_{ab} .

This method shows that time delay estimation is possible without synchronous clocking. Based on the system architecture in Figure 1, the following subsections explore the impact

of the TH precoding and the correlation procedure on ranging accuracy.

2.1. TH precoding with channel knowledge

Since preequalization and correlator performance play critical roles in the distance measurement, the performance of the TH precoding in sensor B and the correlator output of sensor A are analyzed to help understand the behavior of the method. The precoder structure is shown in Figure 3. The modulo operation $Q_I(\cdot)$ is defined as $Q_I(a) = a + b$, where b is the unique integer multiple of I for which $Q_I(a) \in (-I/2, I/2]$. Assuming that the channel impulse response $H(Z)$ is an m th order FIR filter, the approximation of the estimated channel impulse response $\hat{H}(Z)$ is given by

$$\hat{H}(Z) = \sum_{n=0}^{m-1} \hat{g}_n Z^{-n} \simeq \sum_{n=0}^{m-1} (g_n + \Delta g_n) Z^{-n}, \quad (2)$$

where g_n and \hat{g}_n are the coefficients of channel impulse response $H(Z)$ and estimated channel impulse response $\hat{H}(Z)$, respectively. Note that the difference Δg_n between g_n and \hat{g}_n depends on channel estimation errors.

According to Figure 3, the output of the modulo operation $X_k(Z)$ in sensor B is

$$\begin{aligned} X_k(Z) &= S_k(Z) + X_k(Z)(1 - \hat{H}(Z)) - l_k I \\ &= \frac{S_k(Z) - l_k I}{\hat{H}(Z)}, \end{aligned} \quad (3)$$

where l_k is an integer. Therefore, the received signal $P_k(Z)$ in sensor A is

$$\begin{aligned} P_k(Z) &= X_k(Z)H(Z) + N_k(Z) \\ &= (S_k(Z) - l_k I) \cdot \frac{H(Z)}{\hat{H}(Z)} + N_k(Z) \\ &= (S_k(Z) - l_k I) \cdot \frac{\sum_{n=0}^{m-1} g_n Z^{-n}}{\sum_{n=0}^{m-1} \hat{g}_n Z^{-n}} + N_k(Z), \end{aligned} \quad (4)$$

where $N_k(Z)$ is the received noise.

As a result of modulo reduction and providing that the magnitude of the input data and I are chosen such that $\hat{S}_k(Z) \simeq P_k(Z)$, the data output is

$$\hat{S}_k(Z) \simeq P_k(Z) \pmod{I} \quad (5)$$

$$\simeq S_k(Z) \cdot \frac{\sum_{n=0}^{m-1} g_n Z^{-n}}{\sum_{n=0}^{m-1} \hat{g}_n Z^{-n}} + N'_k(Z) \quad (6)$$

$$= S_k(Z) \cdot \sum_{n=0}^{\infty} c_n Z^{-n} + N'_k(Z), \quad (7)$$

where

$$c_n = \begin{cases} \frac{g_0}{\hat{g}_0}, & n = 0 \\ \frac{(g_n - \sum_{j=1}^n \hat{g}_j c_{n-j})}{\hat{g}_0}, & n \geq 1. \end{cases} \quad (8)$$

Note that the coefficient c_n can be shown to be bounded in terms of the estimation errors using mathematical induction. Hence, there exists an upper bound δ for tap gain errors caused by channel estimation errors and an upper bound B for c_n ($n \geq 1$), which is multiple of $\delta/|\hat{g}_0|$.

By optimal L_2 finite impulse response (FIR) approximation [39], a discrete infinite impulse response (IIR) which is analytic in $\{|z| > \rho, \rho < 1\}$ (i.e., possessing a power series in Z^{-1} convergent on the unit circle),

$$F(Z) = \sum_{n=0}^{\infty} f_n Z^{-n} \quad (9)$$

with $f_n = c_n$, can be approximated by a discrete q -coefficient finite impulse response (denoted by FIR(q))

$$\hat{F}(Z) = \sum_{n=0}^{q-1} \hat{f}_n Z^{-n}, \quad (10)$$

where $\hat{f}_n = c_n$.

Given a high SNR and small channel estimation errors, the coefficient c_0 in (8) is approaching one such that the signal term is dominant in (7). Therefore, the noise may be assumed to be negligible in this case. Therefore, based on (10), the data output $\hat{S}_k(Z)$ can be further approximated by

$$\hat{S}_k(Z) \simeq S_k(Z) \cdot \sum_{n=0}^{q-1} c_n Z^{-n}. \quad (11)$$

Then the correlator output of sensor A, r_A , is given by

$$\begin{aligned} r_A &= \int_0^{MT_c} \sum_{n=0}^{q-1} c_n s(t - nT_c) s(t) dt \\ &= MT_c + \sum_{n=1}^{q-1} c_n \int_0^{MT_c} s(t - nT_c) s(t) dt \\ &= MT_c + \sum_{n=1}^{q-1} c_n R_A^n, \end{aligned} \quad (12)$$

where

$$R_A^n = \int_0^{MT_c} s(t - nT_c) s(t) dt. \quad (13)$$

From the derivation in [40–43], the distribution of R_A^n is given by

$$R_A^n \sim \mathcal{N}(0, MT_c(1 - 2|\varepsilon_n| + 2\varepsilon_n^2)), \quad (14)$$

where $\varepsilon_n = (\Delta\tau/T_c) \pm N_\varepsilon T_c$ denotes the normalized fractional timing offset between the two training sequences for the n th component. Note that N_{ε_n} is the smallest integer such that $\varepsilon_n \in (-1, 1)$. Therefore, given the channel information, the distribution of r_A is

$$r_A \sim \mathcal{N}(\mu_{r_A}, \sigma_{r_A}^2), \quad (15)$$

where $\mu_{r_A} = MT_c$ and $\sigma_{r_A}^2 = \sum_{n=1}^{q-1} c_n^2 MT_c(1 - 2|\varepsilon_n| + 2\varepsilon_n^2)$. Hence, as channel estimation errors approach zero (i.e., $B, \delta \rightarrow 0$), we have

$$\lim_{B, \delta \rightarrow 0} r_A = MT_c. \quad (16)$$

With the TH precoding in sensor B, the correlator output r_A converges to MT_c when the channel estimation errors approach zero. On the other hand, without precoding in sensor B, the distribution of r_A can be expressed by the same form as in (15) with $c_n = g_n$. Clearly, the precoding greatly reduces the variance in the correlator output.

2.2. Analysis of ranging accuracy

The fundamental limitation on the ranging accuracy of the estimates is related to the form of the signal and the clock, including signal bandwidth, signal-to-noise ratio (SNR), and timing calibration. Assume that the random range error and range bias error from propagation conditions are negligible. The range-measurement accuracy may be characterized by the measurement error

$$\sigma_R = (\sigma_S^2 + \sigma_{\text{clock}}^2)^{1/2}, \quad (17)$$

where σ_S is the SNR-dependent random ranging accuracy and σ_{clock} is the clock-dependent random ranging accuracy. Note that σ_S relates the accuracy of synchronous distance estimates to the signal-to-noise ratio and the effective bandwidth of the signal. The expression of σ_{clock} is the added inaccuracy due to the asynchronous clocking mechanism.

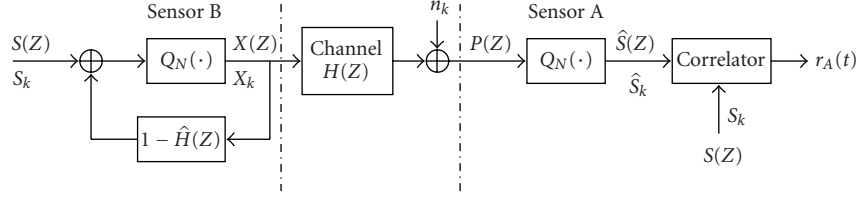


FIGURE 3: Tomlinson-Harashima precoding and linearized description.

2.2.1. Clock-dependent ranging accuracy

Suppose that sensors A and B are equipped with clocks that are asynchronous in both frequency and phase. The random variable T denotes the sensor estimate of the true t ; thus T_{ab} is an estimate of the true time t_{ab} and T_i^A is an estimate of the time t_i^A as measured by the clock of sensor A. From Figure 1, the estimated transmission time is

$$T_{ab} = \frac{T_5^A - T_{\text{del}}^A - T_1^A - T_{\text{obs}}^A}{2}, \quad (18)$$

where $T_{\text{del}}^A = Z \cdot T_{\text{del}}^B$, $T_{\text{del}}^B = T_{\text{pro}}^B + T_{\text{obs}}^B$, and $Z = (T_1^A - T_0^A)/(T_3^B - T_2^B)$. Note that all measurements T_i^A and T_j^B are assumed to be independent normal random variables with the same variance σ^2 caused by the measurement error in the clock. This normality assumption is justified in [44] when the clock skew is small. Z is a scale factor that represents how much faster or slower clock A moves than clock B; T_{obs}^A and T_{obs}^B are the estimated observation time of the correlators in sensors A and B with distributions $\mathcal{N}(t_{\text{obs}}^A, \sigma_{T_{\text{obs}}^A}^2)$ and $\mathcal{N}(t_{\text{obs}}^B, \sigma_{T_{\text{obs}}^B}^2)$, respectively; T_{pro}^B is the estimated processing time of the TH precoder in sensor B with distribution $\mathcal{N}(t_{\text{pro}}^B, \sigma_{T_{\text{pro}}^B}^2)$. Since $\sigma_{T_{\text{obs}}^A}^2$, $\sigma_{T_{\text{obs}}^B}^2$, and $\sigma_{T_{\text{pro}}^B}^2$ are related to the timing resolution of the clock, we may further express $\sigma_{T_{\text{obs}}^A}^2$, $\sigma_{T_{\text{obs}}^B}^2$, and $\sigma_{T_{\text{pro}}^B}^2$ as the variance $2\sigma^2$. Thus, the distribution of the estimated delay time T_{del}^B is given by $T_{\text{del}}^B \sim \mathcal{N}(\mu_{T_{\text{del}}^B}, \sigma_{T_{\text{del}}^B}^2)$, where $\mu_{T_{\text{del}}^B} = t_{\text{pro}}^B + t_{\text{obs}}^B = t_{\text{del}}^B$ and $\sigma_{T_{\text{del}}^B}^2 = \sigma_{T_{\text{pro}}^B}^2 + \sigma_{T_{\text{obs}}^B}^2 = 4\sigma^2$. Since the measurement errors are small, which are the proper conditions for the Gaussian approximation derived in [45–47], the distribution of T_{del}^A is

$$T_{\text{del}}^A \sim \mathcal{N}(\mu_Z \mu_{T_{\text{del}}^B}, 4\mu_Z^2 \sigma^2 + t_{\text{del}}^B{}^2 \sigma_Z^2). \quad (19)$$

Therefore, the distribution of T_{ab} can be sensibly approximated by

$$T_{ab} \sim \mathcal{N}(\mu_{T_{ab}}, \sigma_{T_{ab}}^2), \quad (20)$$

where $\mu_{T_{ab}} = (1/2)(t_5^A - \mu_Z t_{\text{del}}^B - t_1^A - t_{\text{obs}}^A)$ and $\sigma_{T_{ab}}^2 = (1/4)[(4 + 4\mu_Z^2)\sigma^2 + t_{\text{del}}^B{}^2 \sigma_Z^2]$. Thus, the clock-dependent ranging accuracy σ_{clock} is given by

$$\sigma_{\text{clock}}^2 = \sigma_{T_{ab}}^2 = c^2 \sigma_{T_{ab}}^2. \quad (21)$$

2.2.2. SNR-dependent ranging accuracy

The SNR-dependent ranging accuracy of the distance measurement is influenced by the error sources such as channel

estimation, correlator performance, and signal format. Due to channel estimation errors, sensor B may possess erroneous channel information, which may degrade the performance of the TH precoder. Since the operation of the ARTHP method is complex, in this paper the channel estimation is assumed to be accurate (i.e., the variance of the correlator is negligible and the proper correlation peak is chosen) such that the analysis of the proposed approach can be simplified. In this case, the communication channel reduces to an AWGN channel with direct path only. Accordingly, the accuracy of synchronous distance estimates [48–50] is related to the signal-to-noise ratio, the distance, and the effective bandwidth of the signal, which is given by

$$\sigma_s \geq \frac{c \cdot d_{ab}}{2\beta_e \sqrt{2\text{SNR}}}, \quad (22)$$

where β_e is the effective bandwidth of the signal [50].

Hence, from (21) and (22), the estimation error is

$$\sigma_R = (\sigma_s^2 + \sigma_{\text{clock}}^2)^{1/2} \geq \sqrt{\frac{c^2 d_{ab}^2}{8\beta_e^2 \text{SNR}} + c^2 \sigma_{T_{ab}}^2}. \quad (23)$$

3. ASYNCHRONOUS RANGING VIA UWB

An alternative approach is to use a two-way TOA-based ranging technique with UWB signaling. In standard UWB systems, the preamble of a packet can be used to achieve time synchronization. Considering the cooperation between a pair of sensors, in the ARUWB protocol, time calibration is carried out by bidirectional communication without using preamble patterns to compensate the phase and frequency of a clock.

Suppose that sensors A and B are equipped with clocks (oscillators) that are assumed to be asynchronous in both frequency and phase. Denote t_i^a and t_j^b as the time stamps in sensors A and B, respectively; let t_{del}^a and t_{del}^b be the delay time in sensors A and B, respectively; t_{ab} is the signal propagation time. The estimation of the ARUWB method proceeds as shown in Figure 4.

- (i) Sensor A transmits a message, which is a ranging sequence comprising K symbols and containing the times t_0^a and t_1^a (the times indicated on its clock at the start and the end of the transmission, resp.).
- (ii) Sensor B receives the first symbol at time t_2^b (which is t_{ab} seconds after it is transmitted) and receives the last symbol at time t_3^b .

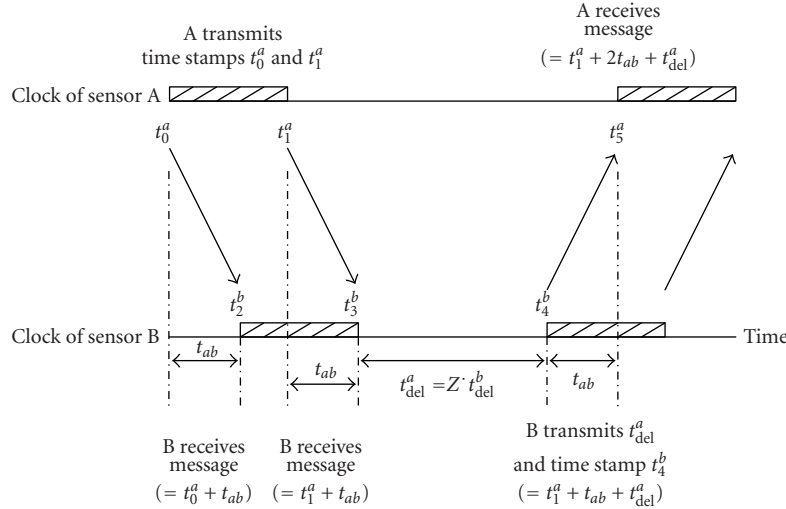


FIGURE 4: The ARUWB method: sensor A receives its reply at t_5^a ; this is equal to $t_1^a + 2t_{ab} + t_{del}^a$, from which A can estimate t_{ab} and hence the distance; in this variation, sensor B can calculate the difference between its clock ($t_3^b - t_2^b$) and A's clock using the time-stamped information in A's messages ($t_1^a - t_0^a$).

- (iii) Sensor B calibrates its clock to A's using the differences $t_1^a - t_0^a$ (which is known from A's message) and $t_3^b - t_2^b$ (the arrival times).
- (iv) Some time t_{del}^a later, sensor B transmits the time $t_4^a = z \cdot t_{del}^b$ that has elapsed since reception of A's message along with the time stamp t_4^b (the time on B's clock when it transmits). These times are adjusted (if necessary) using the scale factor $z = (t_1^a - t_0^a)/(t_3^b - t_2^b)$.
- (v) Sensor A receives the reply from sensor B when its clock reads t_5^a (the time indicated on its clock at the start of the reception). The transmission time t_{ab} can be calculated as

$$t_{ab} = \frac{t_5^a - t_1^a - t_{del}^a}{2}. \quad (24)$$

Notice that the clock calibration is achieved by transmitting a ranging sequence using bidirectional UWB links. Based on the estimation procedures, the ranging performance is analyzed considering clock-dependent estimation accuracy and SNR-dependent estimation accuracy for both AWGN and multipath channels in the following subsections.

3.1. ARUWB in AWGN channels

3.1.1. Clock-dependent ranging accuracy

Referring to Figure 4 and using a Gaussian approximation (which is justified in [45–47]), the distribution of the estimated distance D_{ab} can be well approximated by

$$D_{ab} \sim \mathcal{N}(\mu_{D_{ab}}, \sigma_{D_{ab}}^2) \quad (25)$$

with $\mu_{D_{ab}} = c \cdot \mu_{T_{ab}} = d_{ab}$ and $\sigma_{D_{ab}}^2 = c^2 \sigma_{T_{ab}}^2 = (c^2/4)[(2 + 2\mu_Z^2)\sigma^2 + t_{del}^b \sigma_Z^2]$, where c is the propagation speed of the signal; σ is the timing resolution; μ_Z and σ_Z^2 are the mean and variance of the random variable Z , respectively; $\mu_{T_{ab}}$ and $\sigma_{T_{ab}}^2$

are the mean and variance of the random variable, the transmission time T_{ab} , respectively. Note that the mean of random variable D_{ab} is the true value of the distance between sensors A and B and the variance of D_{ab} depends on the variance of the timing measurement σ , the characteristic of the clock-adjustment factor Z , and the time delay t_{del}^b .

Therefore, the clock-dependent ranging accuracy σ_{clock} is given by

$$\sigma_{clock}^2 = \sigma_{D_{ab}}^2 = c^2 \sigma_{T_{ab}}^2, \quad (26)$$

which is derived as in (25).

3.1.2. SNR-dependent ranging accuracy

For ranging applications using UWB signals, in this work the CRLB for UWB signal formats derived in [36] are used to assess the SNR-dependent ranging accuracy. Given a distance d_{ab} and a channel transfer function, the synchronous ranging accuracy is given by

$$\sigma_s \geq \frac{c}{4\pi} \sqrt{\frac{N_0}{2T \int_{f_L}^{f_H} f^2 |H(f, d_{ab})|^2 \text{PSD}_{\text{MASK}}(f) df}}, \quad (27)$$

with channel transfer function

$$H(f, d_{ab}) = \alpha_0(\tau_0, d_{ab}) e^{j2\pi f \tau_0}, \quad (28)$$

where $\alpha_0(\tau_0, d_{ab})$ is the attenuation factor, which depends on both distance and propagation delay and may be determined based on channel characteristics; T is the transmission time; $[f_L, f_H]$ is frequency range of the signal; $\text{PSD}_{\text{MASK}}(f)$ is the power emission mask. Note that in this paper $\text{PSD}_{\text{MASK}}(f)$ is assumed to be a constant equal to $G_0 = -41.3$ dbm/MHz as regulated by the FCC [36].

For the purpose of comparison, an ideal channel with a transfer function independent of frequency and dependent

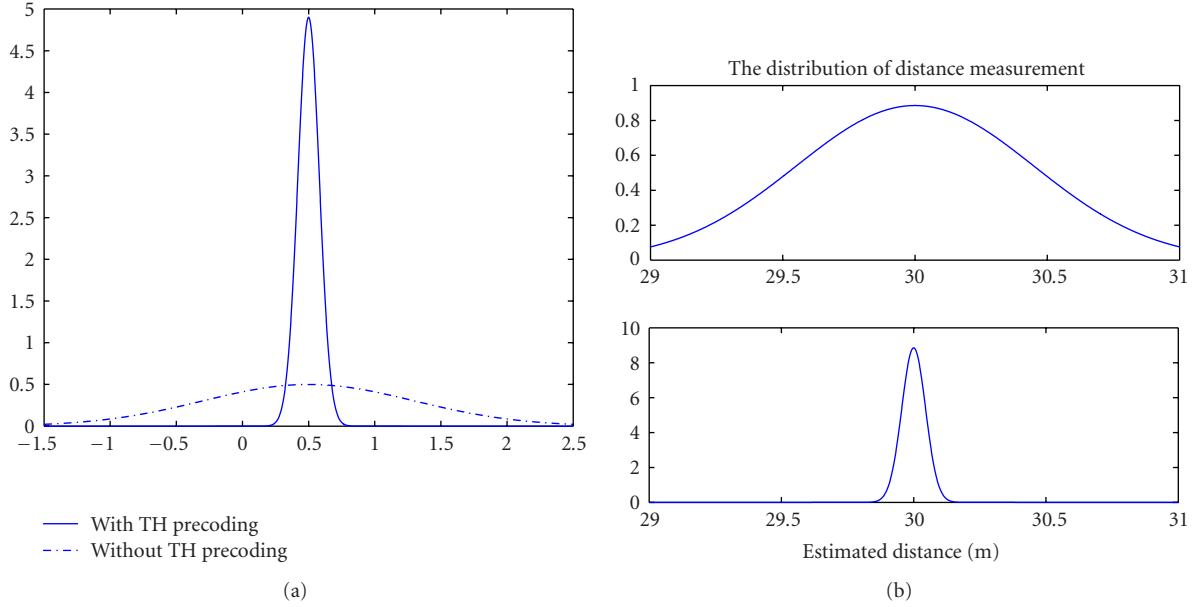


FIGURE 5: The distributions of correlator outputs of sensor A with/without TH precoding (15) with the timing offset $\Delta\tau = 0.5T_c$, $MT_c = 0.5$, and $q = 10$ (left); the distribution of distance measurement in multipath channels using TH precoding (23) with a timing resolution of 1 ns (right top) and 0.1 nanosecond (right bottom): $q = 10$, $t_{ab} = 10^{-7}$, $t_4^b = 3$, $t_3^b = 2$, $t_{obs}^A = 0.2$, $t_2^b = 1.25$, $t_1^a = 0.75$, and $t_0^b = 0.25$ second.

upon distance between transmitter and receiver as the inverse of the square of distance d_{ab} is considered to evaluate the sensitivity of the ranging performance to the multipath effect. Equation (22) therefore can be further expressed as

$$\sigma_S \geq \frac{c \cdot d_{ab}}{4\pi} \sqrt{\frac{3N_0}{2TG_0(f_H^3 - f_L^3)}} \quad (29)$$

with the effective bandwidth of the signal

$$\beta_e = \sqrt{\frac{3}{4\pi^2 T(f_H^3 - f_L^3)}}, \quad (30)$$

where T is equal to $(t_1^a - t_0^a)$, $N_0 = 2.935 \times 10^{-11}$ W/Hz, $G_0 = 7.413 \times 10^{-14}$ W/Hz, and f_H and f_L are the highest and lowest frequency of UWB frequency bands, respectively. Note that the ranging accuracy in different UWB signal formats are related to the difference in bandwidth and the center frequency.

Thus, for an ideal channel, the estimation error σ_R , given by the root-sum-square of the error components, is

$$\sigma_R = (\sigma_S^2 + \sigma_{\text{clock}}^2)^{1/2} \geq \sqrt{\frac{3N_0 c^2 d_{ab}^2}{32\pi^2 T G_0 (f_H^3 - f_L^3)} + c^2 \sigma_{T_{ab}}^2}. \quad (31)$$

3.2. ARUWB in multipath channels

3.2.1. Clock-dependent ranging accuracy

In multipath channels, the time stamp of the received signal is determined by the timing resolution and the propaga-

tion delay. Applying the Gaussian approximation, the distribution of the estimated distance D_{ab} is

$$D_{ab} \sim N(\mu_{D_{ab}}, \sigma_{D_{ab}}^2) \quad (32)$$

with $\mu_{D_{ab}} = c \cdot (\mu_{T_{ab}} + \tau_l) = d_{ab} + c\tau_l$ and $\sigma_{D_{ab}}^2 = c^2 \sigma_{T_{ab}}^2 = (c^2/4)[(2+2\mu_Z^2)\sigma^2 + t_{\text{del}}^b \sigma_Z^2]$, where τ_l is the propagation delay of the l th multipath component. Again the clock-dependent ranging accuracy σ_{clock} is

$$\sigma_{\text{clock}}^2 = \sigma_{D_{ab}}^2 = c^2 \sigma_{T_{ab}}^2. \quad (33)$$

Observe that when the LOS path is significantly attenuated, the distance measurement might be biased by an incorrect choice of multipath component as derived in (32). On the other hand, given a signal with a large SNR and bandwidth in an environment with a dominant LOS path and moderate multipath, the estimated propagation time may be unbiased with a correct choice of the signal arrival time such that the clock-dependent ranging accuracy in multipath channels is close to that in AWGN channels. Thus, the above analysis suggests that in a strong multipath environment, the clock-dependent ranging accuracy might be dominated by the multipath effect instead of the timing resolution as in AWGN channels.

3.2.2. SNR-dependent ranging accuracy

Based on (27), the synchronous ranging accuracy can be further derived as

$$\sigma_S \geq \frac{c \cdot d_{ab}}{4\pi} \sqrt{\frac{3N_0}{2TG_0(f_H^3 - f_L^3)}} \cdot \eta, \quad (34)$$

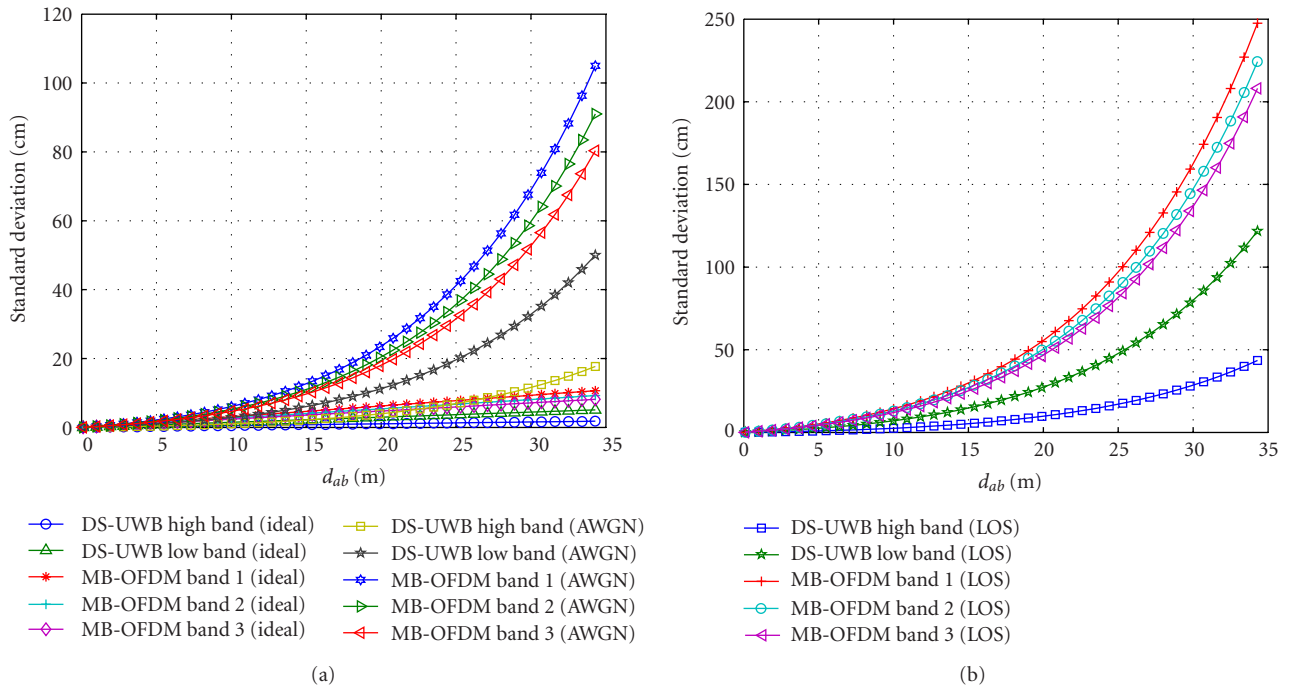


FIGURE 6: The synchronous ranging accuracy of the ARUWB method with fixed observation time $T = 1.83$ microseconds and varying distance d_{ab} (from the first perspective) in ideal and AWGN channels (29) (left) and a multipath channel with a dominant LOS path (34) (right).

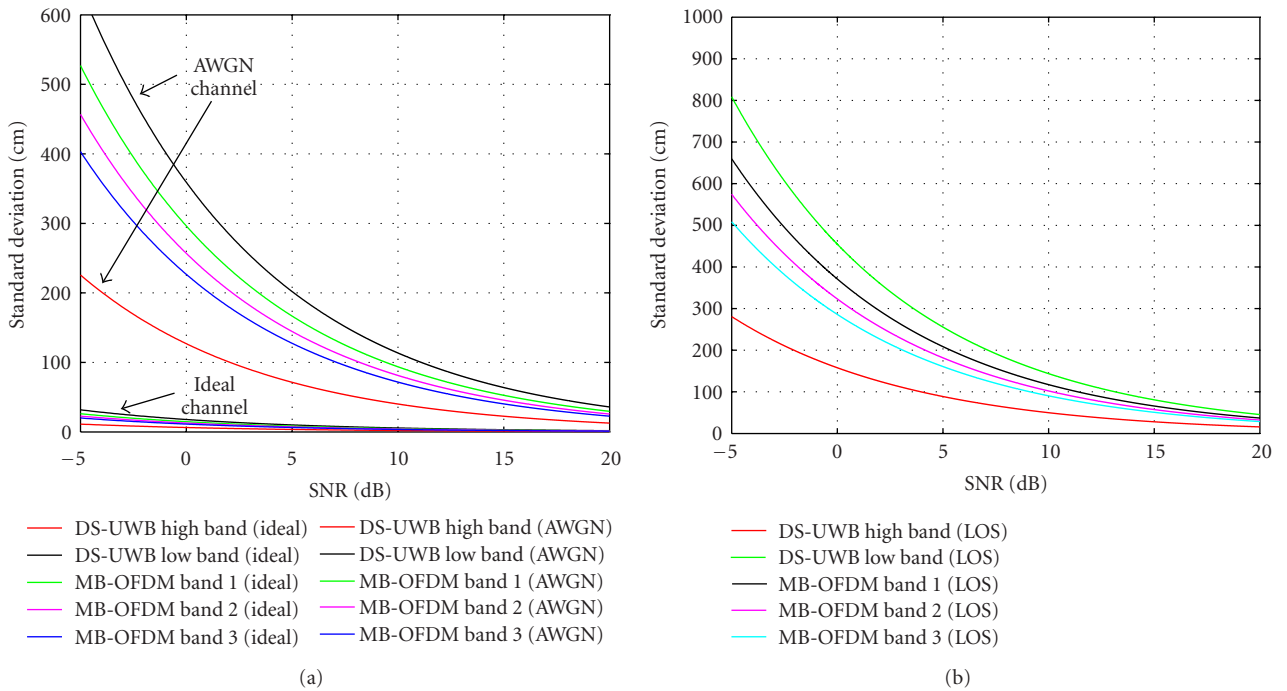


FIGURE 7: The synchronous ranging accuracy of the ARUWB method with fixed distance $d_{ab} = 30$ m and varying SNR (from the second perspective) in ideal and AWGN channels (29) (left) and a multipath channel with a dominant LOS path (34) (right).

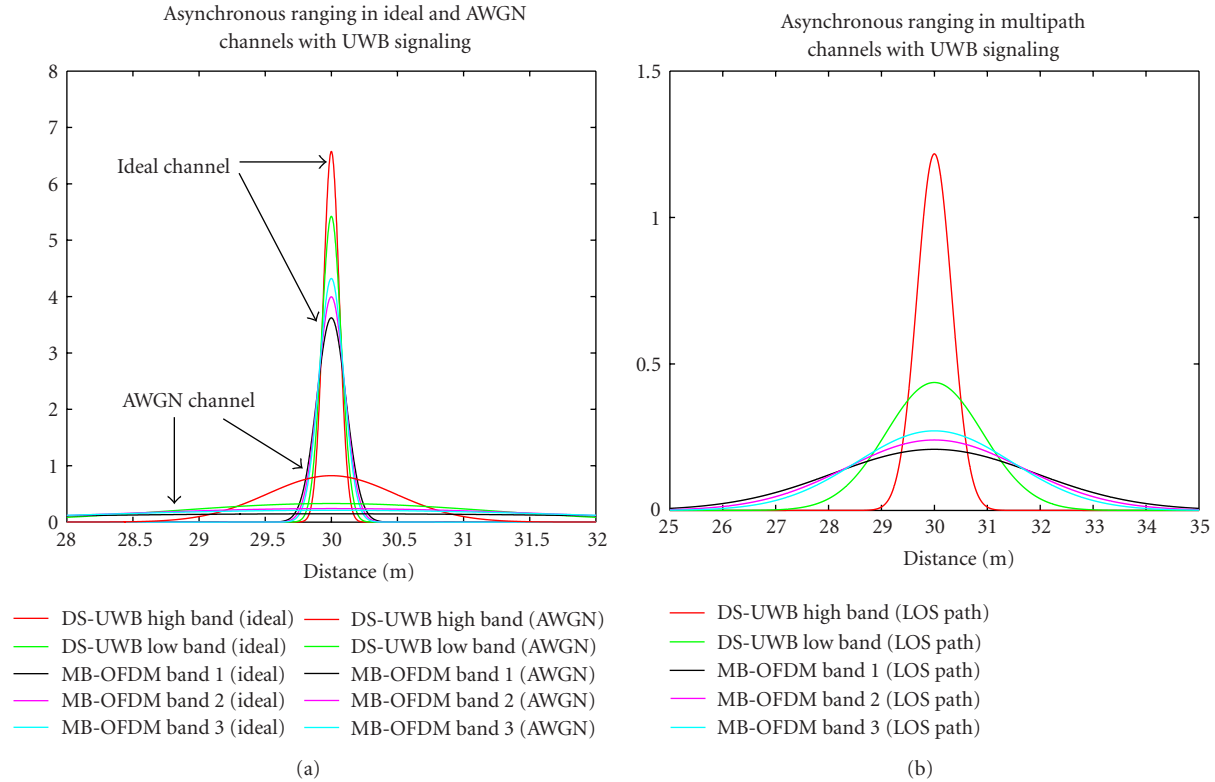


FIGURE 8: The distribution of asynchronous distance measurement using the ARUWB method with a timing resolution of 0.1 nanosecond: $t_{ab} = 10^{-7}$, $t_4^b = 0.3 + 2.92 \mu\text{s}$, $t_3^b = 0.3 + 1.92 \mu\text{s}$, $t_2^b = 0.3$, $t_1^a = 0.25 + 1.83 \mu\text{s}$, and $t_0^a = 0.25$, in ideal and AWGN channels (31) (left) and a multipath channel with a dominant LOS path (37) (right).

where

$$\eta = \frac{1}{d_{ab}} \cdot \sqrt{\frac{\int_{f_L}^{f_H} f^2 \text{PSD}_{\text{MASK}}(f) df}{\int_{f_L}^{f_H} f^2 |H(f, d_{ab})|^2 \text{PSD}_{\text{MASK}}(f) df}} \quad (35)$$

with channel transfer function

$$H(f, d_{ab}) = \sum_{k=0}^{N-1} \alpha_k(\tau_k, d_{ab}) e^{j2\pi f \tau_k}. \quad (36)$$

Observe that the first term in (34) is the SNR-dependent ranging accuracy in an ideal channel and the second term η can be considered as the performance loss due to the multipath effect, which is examined via numerical studies in Section 4.

From (33) and (34), the measurement error σ_R can be expressed as follows:

$$\sigma_R = (\sigma_S^2 + \sigma_{\text{clock}}^2)^{1/2} \geq \sqrt{\frac{3N_0 c^2 d_{ab}^2}{32\pi^2 T G_0 (f_H^3 - f_L^3)} \cdot \eta^2 + c^2 \sigma_{T_{ab}}^2}. \quad (37)$$

4. SIMULATION AND NUMERICAL RESULTS

This section demonstrates the performance of the proposed distance measurement algorithms. Assume that the propagation time is $t_{ab} = 10^{-7}$ s (i.e., the true distance is $d_{ab} = 30$ m) for all distance measurement settings.

The first set of experiments evaluates the performance of the distance measurement using channel estimation with TH precoding. Note that the choice of the $\{t_i^a, t_j^b\}$ values is purely arbitrary in order to show that the proposed technique is able to joint synchronization and ranging with two-way communications. Figure 5(left) depicts the corresponding correlator output of sensor A. Observe that the correlator output r_A without pre-equalization may have larger variance than with TH precoding due to the multipath effects.

Assume the transmitted waveform is a simple rectangular pulse with a zero phase characteristic,

$$a(t) = \text{rect}\left(\frac{t}{t_p}\right), \quad (38)$$

where t_p is the pulse width. In our case, $t_p = T_c$. Figure 5(right) shows the typical performance of the asynchronous bidirectional distance measurement scheme using TH precoding in multipath channels with the parameters detailed in the caption and the clocks providing a resolution based on the symbol rates of the training sequence, 1 Giga-symbol per second (Gsps) (i.e., 1 nanosecond) and 10 Gsps (i.e., 0.1 nanosecond), respectively. Observe that as the distance $d_{ab} = 30$ m, the σ_{ab} is about 6 cm with a timing resolution 0.1 nanosecond. Note that an accurate clock with complicated hardware is required for distance estimation using a

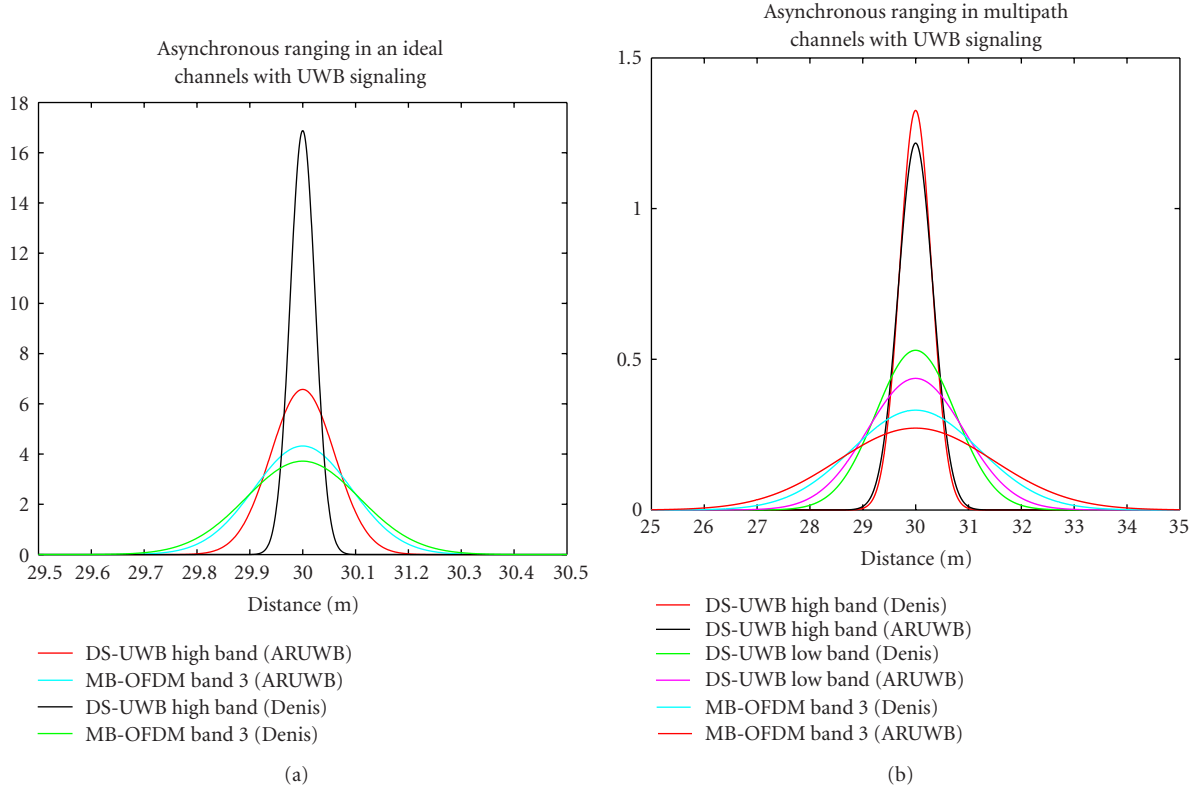


FIGURE 9: The comparison of the asynchronous distance measurement applying the ARUWB method (using (31) and (37)) with the same settings in Figure 8 and the UWB ranging solution in [37] (using (11) and (17)), in ideal and AWGN channels (left) and a multipath channel with a dominant LOS path (right).

higher symbol rate (higher timing resolution) though providing a higher measurement accuracy.

The second set of experiments examines the performance of the ARUWB method in both AWGN and multipath channels with synchronous clocking. The purpose of these experiments is to explore the influence of multipath effects on the ranging performance. The two-ray ground reflection model with the same parameters used in the ARTHP method is considered to evaluate the corresponding measurement errors. Two perspectives are investigated to compare the ranging accuracy using different UWB signal formats: (1) ranging accuracy with fixed observation time T and varying distance d_{ab} ; (2) ranging accuracy with fixed distance d_{ab} and varying observation time T (i.e., with varying SNR). From the first perspective, Figure 6 depicts the synchronous ranging error, which is proportional to the distance between a pair of sensors. Observe that for the UWB signalings, a DS-UWB high-band signal has the best ranging accuracy due to its higher frequency band and larger operation bandwidth and a MB-OFDM Band 1 signal has the worst ranging accuracy because of its lower frequency band and smaller operation bandwidth. As shown in Figure 6, when the distance d_{ab} is equal to 30 m, the standard deviation $\sigma_{d_{ab}}$ of a DS-UWB high-band signal is about 1.8 cm, 12 cm, and 30 cm in ideal (left), AWGN (left), and multipath (right) channels, respectively. Therefore, given time synchronization, the ARUWB

method with DS-UWB High Band signals may be a good approach for ranging.

From the second perspective and (29), note that the estimation error is dominated by the factor $T(f_H^3 - f_L^3)$, which implies that operation frequencies and observation time will determine the estimation accuracy. Given a SNR, MB-OFDM signals have larger observation times compared with DS-UWB signals since the signal energy is given by $E_s = T \cdot \text{PSD}_{\text{MASK}} \cdot (f_H - f_L)$. Figure 7 shows that, again, the proposed method using UWB High Band signals with time synchronization may have better ranging performance in both AWGN (left) and multipath (right) channels.

The third set of experiments studies the performance of the ARUWB method in multipath channels with asynchronous clocking. Since the channel experimental parameters highly depend on the measured environment, in this set of experiments the two-ray ground reflection model is chosen. The parameters for the channel configuration are $\alpha_0 = 0.8$, $\alpha_1 = 0.5$, $\tau_0 = 0$ ns, and $\tau_1 = 5$ ns. Figure 8 illustrates the impact of time synchronization and multipath effects on the distance measurement. Applying the ARUWB method with a DS-UWB High Band signal and given a timing resolution 0.1 ns, the standard deviation $\sigma_{d_{ab}}$ of the estimation is about 30 cm, 50 cm, and 80 cm in ideal (left), AWGN (left) and multipath (right) channels, respectively. Note that though a DS-UWB High Band signal has the best

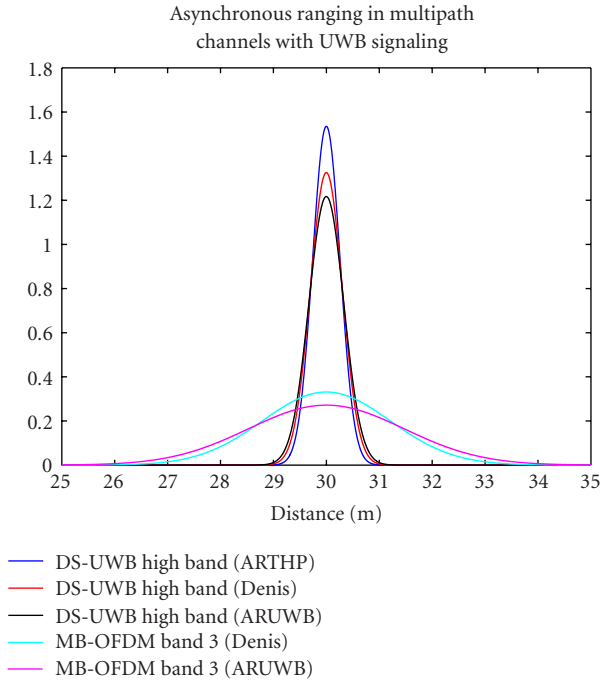


FIGURE 10: The distributions of the distance measurement in a multipath channel with a dominant LOS path using the UWB ranging method in [37, equation (17)], the ARTHP (23), and ARUWB (37) approaches with UWB signaling given the parameters detailed in the captions of Figures 8 and 9.

ranging accuracy in an ideal channel, all of the UWB signal formats have roughly the same estimation performance as shown in Figure 8(left), which implies that the clock-dependent ranging error may dominate the ranging measurement under the circumstances of asynchronous clocking in an ideal channel. However, as shown in Figure 8(right), compared with the clock-dependent ranging error, the SNR-dependent ranging error may dominate estimation performance in multipath channels due to the performance loss caused by multipath effects.

Figure 9 compares the ARUWB method and a UWB ranging solution [37] in an ideal channel and a multipath channel with a dominant LOS path via bi-directional communications. Given the same settings as detailed in the caption of Figure 8 and based on (31) and (37) in Section 3 and [37, equations (11) and (17)] with $W_{\text{LOS}} = 0.61$, $W_{\text{GLOS}} = 1$, $W_{\text{ELOS}} = 0$, $\sigma_{\text{LOS}} = 0.0068$, $W_{\text{NLOS}} = 0.39$, $W_{\text{GNLOS}} = 1$, $W_{\text{ENLOS}} = 0$, and $\sigma_{\text{NLOS}} = 0.0102$ [38], the performance studies show that the measurement results of these two techniques are very closed. It is important to remark that the existing UWB approach [37] considers clock-dependent errors and multipath effects and uses a probabilistic model to describe the weights of different multipath components such that the ranging performance can be investigated based on the channel scenarios. However, many assumptions are made when analyzing the clock-dependent errors and the descriptions of parameter settings, such as how to obtain the SNR-dependent errors and how to set the weights for dif-

ferent multipath components, are not clear. In the ARUWB method, the clock-dependent error is studied and time synchronization mechanism is performed. Moreover, based on the framework in [36], the SNR-dependent errors are further derived under different channel scenarios. Considering the clock-dependent and SNR-dependent estimation errors, the proposed UWB method illustrates a sensible way to assess the ranging performance via bi-directional communications.

For the ARTHP and ARUWB methods, although ranging performance seems to be better in the ARTHP method (with channel information), the performance improvement is achieved at the cost of consuming signal resources for obtaining channel knowledge. Hence, a fair comparison of the proposed techniques with and without channel information requires considering longer signal duration and more signal energy for the ARUWB technique (without channel knowledge). As a result, the following evaluation is made given the same energy consumption in each method. Assume the transmission path is symmetric and the radio dissipates E_{elec} in the transmitter or receiver circuitry and E_{pro} in the information processing. Based on the estimation procedures in the ARTHP method, the radio expends: $E_{\text{ARTHP}} = 6E_{\text{elec(ARTHP)}} + 5E_{\text{pro(ARTHP)}}$, including the operations for communication and signal processing such as signal transmission and reception, channel estimation, correlation, TH precoding, and range-measurement calculation. Similarly, for the ARUWB method, the total energy consumption is $E_{\text{ARUWB}} = 4E_{\text{elec(ARUWB)}} + 2E_{\text{pro(ARUWB)}}$, which is dissipated for signal transmission and reception, timing calibration, and distance estimation. Since computation is much cheaper than communication, we have $E_{\text{ARTHP}} \approx 6E_{\text{elec(ARTHP)}}$ and $E_{\text{ARUWB}} \approx 4E_{\text{elec(ARUWB)}}$, which may decide the relationship between $E_{\text{elec(ARTHP)}}$ and $E_{\text{elec(ARUWB)}}$ for a given energy.

Given the above settings, Figure 10 shows that the performance of the ARTHP method with DS-UWB High Band signals is superior to that of the ARUWB method with different UWB signal formats due to the contributions of multipath to the distance estimations. Note that the ARTHP method does not require any signaling for the ranging task. Compared with the ARUWB method, the system architecture of the ARTHP approach has greater circuitry requirement and computational complexity due to channel estimation and TH precoding. From Figures 6 to 10, observe that under the circumstance of a dominant LOS path, the ARUWB approach may be a good technique for sensor ranging; on the other hand, if the LOS path is attenuated significantly, the ARTHP approach may be preferred since the multipath effect can be canceled out by the preequalization.

5. CONCLUSION

This paper presents two decentralized methods which simultaneously undertake synchronization and ranging based on an asynchronous two-way TOA approach for wireless ad-hoc sensor networks. These asynchronous and cooperative communication procedures may simplify the computational and circuitry complexity of the ranging estimation in each sensor. In order to alleviate the multipath effect,

Tomlinson-Harashima precoding and UWB signaling are used for the distance measurement between pairs of sensors. In the ARTHP technique, an algorithm is presented to cancel the channel effect, which is crucial to the ranging accuracy. In the ARUWB method, the range-measurement accuracy highly benefits from the well-known features of UWB signaling such as in communication and radio-location applications to provide precise time-of-arrival estimates in multipath channels. Sensible settings for the ranging problems using the ARTHP and ARUWB approaches are presented and the proposed mechanisms are simulated and analyzed to assess the accuracy of the distance estimation. Depending on the measurement accuracy, the parameters in each technique can be determined to achieve desired performance.

For the two proposed ranging solutions, tradeoffs are found between model complexity, energy consumption, computational complexity, and sensible model description in real systems. Future plans will involve generalizing the methods to consider certain failure scenarios and to explore the sensitivity of the proposed schemes to system models and network operation.

REFERENCES

- [1] A. Savvides, M. Srivastava, L. Girod, and D. Estrin, "Localization in sensor networks," in *Wireless Sensor Networks*, C. R. Raghavendra, K. M. Sivalingam, and T. Znati, Eds., Kluwer Academic, New York, NY, USA, 2004.
- [2] R. Iyengar and B. Sikdar, "Scalable and distributed GPS free positioning for sensor networks," in *Proceedings of the IEEE International Conference on Communications (ICC '03)*, vol. 1, pp. 338–342, Anchorage, Alaska, USA, May 2003.
- [3] T. Kitasuka, T. Nakanishi, and A. Fukuda, "Location estimation system using wireless ad-hoc network," in *Proceedings of the 5th International Symposium on Wireless Personal Multimedia Communications (WPMC '02)*, vol. 1, pp. 305–309, Honolulu, Hawaii, USA, October 2002.
- [4] R. Govindan, T. Faber, J. Heidemann, D. Estrin, et al., "Ad hoc smart environments," in *Proceedings of the DARPA/NIST Workshop on Smart Environments*, Atlanta, Ga, USA, June 1999.
- [5] H. Wang, J. Elson, L. Girod, D. Estrin, K. Yao, and L. Vanderberge, "Target classification and localization in habitat monitoring," in *Proceedings of IEEE International Conference on Acoustics, Speech and Signal Processing (ICASSP '03)*, pp. 597–600, Hong kong, April 2003.
- [6] A. H. Sayed, A. Tarighat, and N. Khajehnouri, "Network-based wireless location: challenges faced in developing techniques for accurate wireless location information," *IEEE Signal Processing Magazine*, vol. 22, no. 4, pp. 24–40, 2005.
- [7] N. B. Priyantha, A. Chakraborty, and H. Balakrishnan, "The cricket location-support system," in *Proceedings of the 6th Annual International Conference on Mobile Computing and Networking (MOBICOM '00)*, pp. 32–43, Boston, Mass, USA, August 2000.
- [8] A. Savvides, C.-C. Han, and M. B. Srivastava, "Dynamic fine-grained localization in ad-hoc networks of sensors," in *Proceedings of the 7th Annual International Conference on Mobile Computing and Networking (MOBICOM '01)*, pp. 166–179, Rome, Italy, July 2001.
- [9] A. Savvides, H. Park, and M. B. Srivastava, "The bits and flops of the n-hop multilateration primitive for node localization problems," in *Proceedings of the 1st ACM International Workshop on Wireless Sensor Networks and Applications (WSNA '02)*, pp. 112–121, Atlanta, Ga, USA, September 2002.
- [10] D. Niculescu and B. Nath, "Ad hoc positioning system (APS) using AOA," in *Proceedings of the 22nd Annual Joint Conference on the IEEE Computer and Communications Societies (INFOCOM '03)*, vol. 3, pp. 1734–1743, San Francisco, Calif, USA, March-April 2003.
- [11] Y. Shang, J. Meng, and H. Shi, "A new algorithm for relative localization in wireless sensor networks," in *Proceedings of the 18th International Parallel and Distributed Processing Symposium (IPDPS '04)*, vol. 18, p. 24, Santa Fe, NM, USA, April 2004.
- [12] F. Gustafsson and F. Gunnarsson, "Mobile positioning using wireless networks: possibilities and fundamental limitations based on available wireless network measurements," *IEEE Signal Processing Magazine*, vol. 22, no. 4, pp. 41–53, 2005.
- [13] A. Nasipuri and K. Li, "A directionality based location discovery scheme for wireless sensor networks," in *Proceedings of the 1st ACM International Workshop on Wireless Sensor Networks and Applications (WSNA '02)*, pp. 105–111, Atlanta, Ga, USA, September 2002.
- [14] C.-Y. Wen, R. D. Morris, and W. A. Sethares, "Distance estimation using bidirectional communications without synchronous clocking," *IEEE Transactions on Signal Processing*, vol. 55, no. 5, pp. 1927–1939, 2007.
- [15] L. J. Greenstein, J. B. Andersen, H. L. Bertoni, S. Kozono, D. G. Michelson, and W. H. Tranter, Eds., "Channel and propagation models for wireless system design I," *IEEE Journal on Selected Areas in Communications*, vol. 20, no. 3, pp. 493–495, 2002.
- [16] L. J. Greenstein, J. B. Andersen, H. L. Bertoni, S. Kozono, D. G. Michelson, and W. H. Tranter, Eds., "Channel and propagation models for wireless system design II," *IEEE Journal on Selected Areas in Communications*, vol. 20, no. 6, 2002.
- [17] M. Tomlinson, "New automatic equaliser employing modulo arithmetic," *Electronics Letters*, vol. 7, no. 5-6, pp. 138–139, 1971.
- [18] M. V. Eyuboglu, G. D. Forney Jr., P. Dong, and G. Long, "Advanced modulation techniques for V.fast," *European Transactions on Telecommunications*, vol. 4, no. 3, pp. 243–256, 1993.
- [19] R. Laroia, S. A. Tretter, and N. Farvardin, "Simple and effective precoding scheme for noise whitening on intersymbol interference channels," *IEEE Transactions on Communications*, vol. 41, no. 10, pp. 1460–1463, 1993.
- [20] A. Narula, M. J. Lopez, M. D. Trott, and G. W. Wornell, "Efficient use of side information in multiple-antenna data transmission over fading channels," *IEEE Journal on Selected Areas in Communications*, vol. 16, no. 8, pp. 1423–1436, 1998.
- [21] E. Visotsky and U. Madhow, "Space-time transmit precoding with imperfect feedback," *IEEE Transactions on Information Theory*, vol. 47, no. 6, pp. 2632–2639, 2001.
- [22] G. Jongren, M. Skoglund, and B. Ottersten, "Combining beamforming and orthogonal space-time block coding," *IEEE Transactions on Information Theory*, vol. 48, no. 3, pp. 611–627, 2002.
- [23] S. Zhou and G. B. Giannakis, "Optimal transmitter eigenbeamforming and space-time block coding based on channel mean feedback," *IEEE Transactions on Signal Processing*, vol. 50, no. 10, pp. 2599–2613, 2002.
- [24] F. Rey, M. Lamarca, and G. Vazquez, "Robust power allocation algorithms for MIMO OFDM systems with imperfect CSI," *IEEE Transactions on Signal Processing*, vol. 53, no. 3, pp. 1070–1085, 2005.

- [25] A. P. Liavas, "Tomlinson-Harashima precoding with partial channel knowledge," *IEEE Transactions on Communications*, vol. 53, no. 1, pp. 5–9, 2005.
- [26] O. Simeone, Y. Bar-Ness, and U. Spagnolini, "Linear and nonlinear preequalization/equalization for MIMO systems with long-term channel state information at the transmitter," *IEEE Transactions on Wireless Communications*, vol. 3, no. 2, pp. 373–378, 2004.
- [27] S. Gezici, Z. Tian, G. B. Giannakis, et al., "Localization via ultra-wideband radios: a look at positioning aspects of future sensor networks," *IEEE Signal Processing Magazine*, vol. 22, no. 4, pp. 70–84, 2005.
- [28] S. Gezici, Z. Sahinoglu, H. Kobayashi, H. Poor, and A. Molisch, "A two-step time of arrival estimation algorithm for impulse radio ultra wideband systems," Tech. Rep. TR2005-028, Mitsubishi Electric Research Laboratories, Cambridge, Mass, USA, December 2005.
- [29] B. Denis, J. Keignart, and N. Daniele, "Impact of NLOS propagation upon ranging precision in UWB systems," in *Proceedings of IEEE Conference on Ultra Wideband Systems and Technologies (UWBST '03)*, pp. 379–383, Reston, Va, USA, November 2003.
- [30] C. Falsi, D. Dardari, L. Mucchi, and M. Z. Win, "Time of arrival estimation for UWB localizers in realistic environments," *EURASIP Journal on Applied Signal Processing*, vol. 2006, Article ID 32082, 13 pages, 2006.
- [31] J.-Y. Lee and R. A. Scholtz, "Ranging in a dense multipath environment using an UWB radio link," *IEEE Journal on Selected Areas in Communications*, vol. 20, no. 9, pp. 1677–1683, 2002.
- [32] J. Zhang, R. A. Kennedy, and T. D. Abhayapala, "Cramér-Rao lower bounds for the synchronization of UWB signals," *EURASIP Journal on Applied Signal Processing*, vol. 2005, no. 3, pp. 426–438, 2005.
- [33] A. Batra, J. Balakrishnan, A. Dabakand, et al., "Multi-band OFDM physical layer proposal for IEEE.802.15 Task Group 3a," September 2004.
- [34] R. Fisher, R. Kohno, and M. M. Laughlin, "DS-UWB physical layer submission to 802.15 Task Group 3a," July 2004, <ftp://ieee.wireless@ftp.802wirelessworld.com/15/04/15-04-0137-00-003a-merger2-proposalds-uwb-update.pdf>.
- [35] IEEE 802.15.TG4a, <http://www.ieee802.org/15/pub/TG4a.html>.
- [36] R. Cardinali, L. De Nardis, M.-G. Di Benedetto, and P. Lombard, "UWB ranging accuracy in high- and low-data-rate applications," *IEEE Transactions on Microwave Theory and Techniques*, vol. 54, no. 4, pp. 1865–1875, 2006.
- [37] B. Denis, J.-B. Pierrot, and C. Abou-Rjeily, "Joint distributed synchronization and positioning in UWB ad hoc networks using TOA," *IEEE Transactions on Microwave Theory and Techniques*, vol. 54, no. 4, pp. 1896–1911, 2006.
- [38] B. Denis, J. Keignart, and N. Daniele, "Impact of NLOS propagation upon ranging precision in UWB systems," in *Proceedings of IEEE Conference on Ultra Wideband Systems and Technologies (UWBST '03)*, pp. 379–383, Reston, Va, USA, November 2003.
- [39] P. J. Kootsookos and R. R. Bitmead, "The nehari shuffle and minimax FIR filter design," in *Control and Dynamic Systems, Vol. 64: Stochastic Techniques in Digital Signal Processing Systems*, C. T. Leondes, Ed., Academic Press, New York, NY, USA, 1994.
- [40] W. K. Alem and C. L. Weber, "Acquisition techniques of PN sequences," in *Proceedings of the IEEE National Telecommunications Conference (NTC '77)*, vol. II, pp. 35:2-1–35:2-4, Los Angeles, Calif, USA, December 1977.
- [41] A. Polydoros and C. L. Weber, "Rapid acquisition techniques for direct sequence spread spectrum systems using an analog detector," in *Proceedings of the IEEE National Telecommunications Conference (NTC '81)*, vol. 1, pp. A7. 1. 1–A7. 1. 5, Orleans, La, USA, November 1981.
- [42] A. Polydoros and C. L. Weber, "A unified approach to serial search spread spectrum code acquisition," *IEEE Transactions on Communications*, vol. 32, no. 5, pp. 542–549, 1984.
- [43] M. K. Simon, J. K. Omura, R. A. Scholtz, and B. K. Levitt, *Spread Spectrum Communications*, vol. III, Computer Science Press, Rockville, Md, USA, 1985.
- [44] F. Zhao and L. Guibas, *Wireless Sensor Networks: An Information Processing Approach*, Morgan Kaufmann, San Francisco, Calif, USA, 2004.
- [45] E. C. Fieller, "The distribution of the index in a normal bivariate population," *Biometrika*, vol. 24, no. 3-4, pp. 428–440, 1932.
- [46] D. V. Hinkley, "On the ratio of two correlated normal random variables," *Biometrika*, vol. 56, no. 3, pp. 635–639, 1969.
- [47] R. Ware and F. Lad, "Approximating the distribution for sum of product of normal variables," the research report of the Mathematics and Statistics department at Canterbury University, 2003, <http://www.math.canterbury.ac.nz/research/ucdms2003n15.pdf>.
- [48] V. H. Poor, *An Introduction to Signal Detection and Estimation*, Springer, New York, NY, USA, 2nd edition, 1994.
- [49] W. S. Burdick, *Radar Signal Analysis*, Prentice-Hall, Santa Barbara, Calif, USA, 1968.
- [50] G. R. Curry, *Radar System Performance Modeling*, Artech House, Boston, Mass, USA, 2nd edition, 2005.
- [51] D. C. Cox, R. R. Murray, and A. W. Norris, "800 MHz attenuation measured in and around suburban houses," *AT&T Bell Laboratories Technical Journal*, vol. 673, no. 6, pp. 921–954, 1984.
- [52] R. C. Bernhardt, "Macroscopic diversity in frequency reuse systems," *IEEE Journal on Selected Areas in Communications*, vol. 5, no. 5, pp. 862–878, 1987.
- [53] N. Patwari, A. O. Hero III, M. Perkins, N. S. Correal, and R. J. O'Dea, "Relative location estimation in wireless sensor networks," *IEEE Transactions on Signal Processing*, vol. 51, no. 8, pp. 2137–2148, 2003.

Composition Comments

1. Please provide the corresponding author and his/her e-mail address.
2. We changed "signalling" to the highlighted "signaling" in the main title. Please check similar cases throughout.
3. Please check the accuracy of the highlighted part. Please check similar cases throughout.
4. We split this reference to [15, 16]. Please check.
5. Please note that the URL is not accessible.